

External Strain Induced Semi-metallic and Metallic Phase of Chlorographene

Shivam Puri^{1,*} and Somnath Bhowmick^{1,†}

¹*Department of Material Science and Engineering,
Indian Institute of Technology, Kanpur 208016, India*

(Dated: August 13, 2018)

In order to overcome the limitations of graphene due to lack of intrinsic bandgap, it is generally functionalized with hydrogen or halogen atoms like fluorine and chlorine. Generally, such functionalization yields a moderate to high bandgap material in case of 100% coverage, for example ≈ 1.5 eV in graphene functionalized with chlorine atoms or chlorographene. In this paper, using *ab initio* calculations, we report very interesting transformations observed in chlorographene under external strain, driving it to a state with nearly vanishing bandgap (under tensile strain) and even converting it to a metal (under compressive strain). We also show the importance of spin-orbit coupling, responsible for the few meV bandgap of chlorographene observed under high tensile strain, which would have been a gapless semi-metal otherwise.

The past decade has seen a tremendous growth of two dimensional (2D) materials, with numerous discoveries of atomically thin layers with fascinating properties suitable for applications in next generation electronic, optoelectronic and magnetic devices.¹ The rise of 2D materials started with the first successful isolation of a single layer of graphite, known as graphene.²⁻⁴ Post-discovery, graphene enthralled the researches with its fascinating electronic-transport properties like quantum Hall Effect at room temperature, very high carrier mobility, long mean free path and ballistic transport of electrons.⁴ In addition to this, superior mechanical strength, high thermal conductivity and remarkable flexibility of graphene makes it an ideal candidate for device applications.

The origin of exotic electronic-transport properties of graphene lies in its linear energy dispersion (resembling the Dirac spectrum of massless fermions) at the high-symmetry points located at the six corners (denoted as K points) of the hexagonal Brillouin zone.^{5,6} Since the highest occupied and lowest unoccupied band touches each other at the Dirac points (K points), graphene is classified as a semi-metal. Unfortunately, lack of intrinsic bandgap limits the use of graphene to some extent. For example, the advantage of ultrahigh electron mobility is nullified by high off current in graphene based field effect transistor (FET) devices.

Fabrication of nanoribbons and quantum dots is one possible solution, as bandgap appears due to quantum confinement effect.⁷ Although graphene nanoribbons have several interesting features, like spontaneous spin polarization along the edges, their fabrication with atomically controlled edge shapes remains a challenge.⁸⁻¹⁰ Other alternative is to functionalize graphene via chemical adsorption of hydrogen^{11,12} or halogen atoms like fluorine¹³⁻¹⁶ and chlorine.¹⁷⁻¹⁹ Unfortunately, this leads to a large bandgap of magnitude 3.5-3.7 eV in case of hydrogenation, 2.9-3.1 eV in case of fluorination and 1.2-1.5 eV in case of chlorination, as reported in several computational and experimental studies.¹¹⁻¹⁹ Reducing the bandgap is certainly going to make them more appealing for device applications.

Being atomically thin, 2D materials can not screen the

external fields very effectively. As a result, perturbations like applied strain and electric field are known to significantly change the electronic band structure of 2D materials. For example, in case of MoS₂, experimental studies have reported nearly 100 meV bandgap decrease per percent of applied strain, accompanied by direct-to-indirect transition of the character of the bandgap.^{20,21} Similar predictions have been made for 2D phosphorus allotropes, where applied strain is also found to switch the preferred conduction direction.²²⁻²⁴ Bandgap can also be tuned by applying an electric field in a direction perpendicular to the plane of the 2D material, as shown for MoS₂²⁵⁻²⁷, phosphorene²⁸⁻³¹ and multilayer graphene.³²

In this paper we select chlorographene, which has the lowest bandgap among the functionalized graphene siblings and study the effect of strain (within the elastic limit) on its electronic band structure. We show that, sizeable bandgap of chlorographene can be reduced to a vanishingly small value of a few meV (under tensile strain) and it can even be converted to a metallic state (under compressive strain). We find that spin-orbit coupling is responsible for the few meV bandgap observed under high tensile strain, otherwise which appears like a gapless semi-metallic state of chlorographene. Based on symmetry arguments, we expect the results to be qualitatively true for other materials with same space group symmetry and in that sense, our study is quite general in nature.

Structural optimizations and electronic band structure calculations are carried out using QUANTUM ESPRESSO³⁵ package, implementing density functional theory (DFT) using a plane-wave basis set (kinetic energy cutoff taken to be 80 Ry). Core electrons are treated using the norm-conserving pseudopotentials and exchange-correlation effects are included within the framework of generalized gradient approximations(GGA). A k -point mesh of $24 \times 24 \times 1$ is used to obtain the electron density in a self-consistent manner. Structural optimizations are carried out until the energy difference between two successive steps are less than 10^{-4} Ry and all three components of the force on each atom are less than 10^{-3} Ry/Bohr.

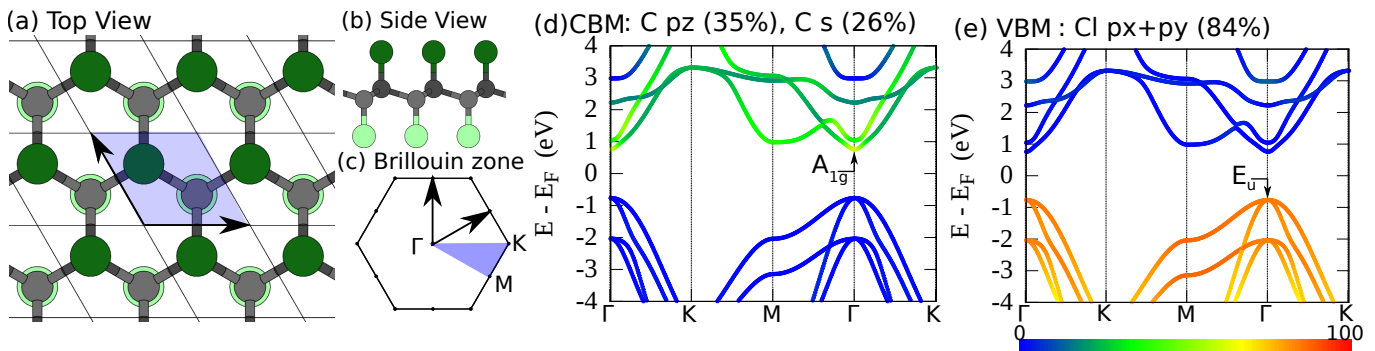


FIG. 1. (a) Top view and (b) side view of chlorographene unit cell and (c) the corresponding high symmetry points in the reciprocal lattice. Carbon and chlorine atoms are shown in black and green, respectively, while the dark and light shading in panels (a) and (b) are done according to the height of the atoms. Crystal structures are prepared by using Xcrystden.^{33,34} Orbital resolved electronic band structure of chlorographene is depicted in (d) and (e), highlighting the major contributions from different atomic orbitals. Panel (d) illustrates the relative weight of C p_z and C s orbital on different energy bands. Panel (e) illustrates the same for Cl p_x and p_y . At the Γ point, VBM (CBM) corresponds to the irreducible representation E_u (A_{1g}) of D_{3d} point group. VBM (E_u) is found to be doubly degenerate.

Graphene has a honeycomb lattice of carbon atoms with a space group symmetry of $P6/mmm$ (#191), which is lowered to $P\bar{3}m1$ (#164) by full chlorination (one Cl atom per C) and the resulting 2D material is known as chlorographene. The crystal structure and hexagonal unit cell of chlorographene is illustrated in Fig 1(a)-(b). Using the computational parameters mentioned above, the lattice constant of fully relaxed structure of chlorographene is measured to be 2.91 Å, while the C-C and C-Cl bond length is found to be 1.75 Å and 1.74 Å, respectively and the C-C-C and C-C-Cl bond angle is obtained to be 111.98° and 106.83°, respectively. The first Brillouin zone of chlorographene is shown in Fig 1(c) and the high symmetry points are marked as Γ (center of the Brillouin zone), K (corner of the Brillouin zone) and M (center of the edges of the Brillouin zone).

The electronic band structure is plotted along the high symmetry lines Γ -K, K-M and M- Γ [see Fig. 1(d)-(e)].³⁶ As shown in the diagram, a direct bandgap at the Γ point, measuring 1.5 eV, is obtained in case of chlorographene, which is in good agreement with the value reported in the literature.¹⁹ It is observed that the valence band maximum (VBM) is two fold degenerate (heavy hole and light hole), while the conduction band minimum (CBM) is non-degenerate. Degeneracy of the hole bands at the Γ point is dictated by symmetry and it is also observed in other 2D materials of $P\bar{3}m1$ space group, like monolayer β phosphorus²² and arsenic,³⁷ as well as blue phosphorus oxide.³⁸ Two states at the VBM (one state at the CBM) corresponds to the irreducible representation E_u (A_{1g}) of D_{3d} point group at the Γ point. When band states are projected on the atomic orbitals, it is found that, close to the Γ point, the valence bands are mostly formed by the p_x and p_y orbital of Cl, while the conduction band edge is constituted mainly by the p_z and s orbitals of C.

Impact of deformation on electronic band structure is investigated by applying compressive (upto 7%) and tensile (upto 13%) strain bi-axially, such that the symmetry

of the pristine material is preserved after contraction or expansion of the unit cell vectors. The strains applied are within the elastic limit predicted for chlorographene, as predicted by *ab initio* calculations.¹⁹ Bi-axial strain upto 6% has so far been reported experimentally in similar 2D materials like MoS₂.²¹ The overall effect of bi-axial strain is summarized in a three dimensional electronic band structure diagram, where only three low energy bands near the valence and conduction band edge of chlorographene are shown for the sake of clarity [see Fig. 2]. In this diagram, we plot the energy level shift (measured with respect to the vacuum energy level) of E_u and A_{1g} states, as a function of applied strain. Clearly, energy level of doubly degenerate E_u states falls with increasing tensile strain, while it rises with increasing compressive strain. In contrast, energy level of A_{1g} states falls with increasing tensile, as well as compressive strain. Due to the energy level shift of E_u and A_{1g} states, bandgap of chlorographene gradually closes with increasing strain, which finally leads to a phase transition. Shaded areas, located extreme right and left of Fig. 2, mark the regions where chlorographene is no longer a semiconductor. Interestingly, phase transition under tensile strain is qualitatively different from what we observe with compressive strain. It is found that, while a semiconductor to semi-metal transition takes place in the tensile region (beyond 12% strain), on the other hand, chlorographene transforms to a metallic state under compression (beyond 6.2% strain). Interestingly, two bands are also found to be touching each other along a circular line surrounding the Γ point in the latter state.

Let us first have a detailed discussion on what happens until the point of phase transition. As long as chlorographene exists as a semiconductor, doubly degenerate E_u states remain at the valence band top, while A_{1g} state prevails at the conduction band bottom. The orbital resolved band structure of chlorographene under tensile strain is shown in Fig 3 (a) and (b). Clearly, near

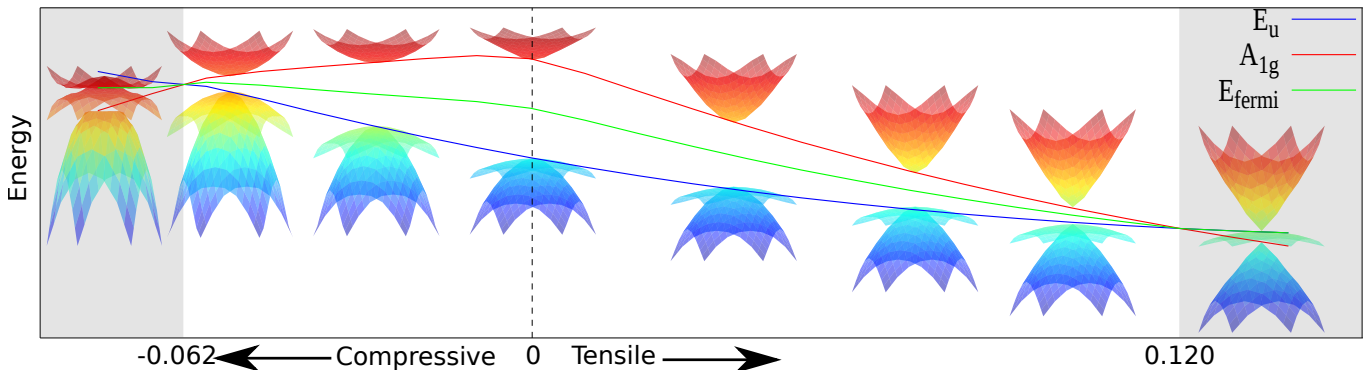


FIG. 2. Effect of strain on band edges of chlorographene is shown. Energy level (measured with respect to the vacuum energy level) of the valence band edge (E_u irreducible representation of D_{3d} point group at the Γ point) falls with increasing tensile strain, while it rises with increasing compressive strain. On the other hand, energy level of the conduction band edge (A_{1g} irreducible representation of D_{3d} point group at the Γ point) falls with increasing tensile, as well as compressive strain. As a result of band edge shifting, bandgap of chlorographene closes gradually with increasing strain, followed by a phase transition (shaded region), which is qualitatively different for tensile and compressive strain. In the tensile side, a semiconductor to semimetal phase transition is observed beyond 12% critical strain, while a semiconductor to metal phase transition is found beyond 6.2% compressive strain.

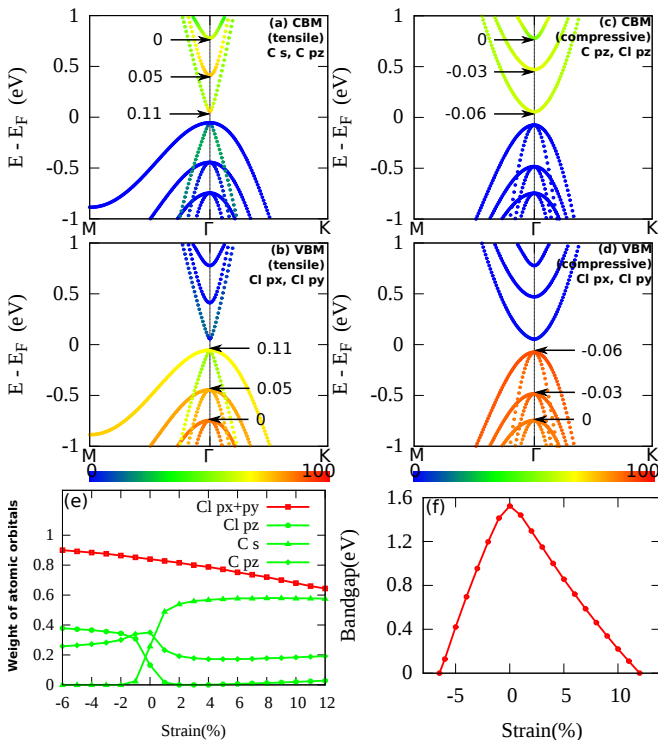


FIG. 3. Orbital resolved band structure of chlorographene is illustrated; under (a)-(b) tensile (0, 5 and 11%) and (c)-(d) compressive (0, 3 and 6%) strain. The corresponding atomic orbitals are mentioned in respective panels. (e) Weight of the atomic orbitals, forming the band edges of chlorographene, is shown as a function of strain. (f) Bandgap of chlorographene is plotted at different values of strain.

the Γ point, the valence band edge is formed by mainly p_x and p_y atomic orbital of Cl. On the other hand, conduction band edge is composed of s and p_z orbital of C. In the same figure, the orbital resolved band structure

of chlorographene under compressive strain is plotted in panel (c) and (d). A thorough comparison reveals that, the valence band edge is still dominated by the p_x and p_y atomic orbital of Cl, similar to the case of chlorographene under tensile strain. However, a significant contribution of p_z orbital of Cl is found near the conduction band edge under compression; instead of s orbital of C, as observed in case of tensile strain. Other than that, p_z orbital of C has a significant weight in case of CBM of chlorographene, both under compression and tension. A summary of relevant atomic orbitals is given in Fig 3 (e) by plotting their weight as a function of strain. Clearly, in equilibrium (zero strain) weight of the atomic orbitals at the CBM is in the following order: $C p_z > C s > Cl p_z$. However, contribution from s orbital of C atom rises and p_z orbital of Cl atom falls rapidly under tensile strain. This is exactly opposite to what happens under compressive strain, where weight of p_z orbital of Cl atom rises to prominence, while it decays to negligible values for s orbital of C atom. The electronic band structures presented in Fig. 3 also clearly illustrates that the bandgap decreases with increasing strain (both compressive and tensile) and it's magnitude is plotted as a function of strain in panel (f) of the same figure. Note that, the bandgap changes more sharply under compressive strain, although ultimately it drops to zero in either case and the particular nature of the phase transition is going to be discussed in the following paragraphs.

First, let us focus on the semi-metallic phase appearing beyond 12% tensile strain. A representative electronic band structure of semi-metallic phase of chlorographene (under 13% tensile strain) is shown in Fig. 4. Clearly, the valence band top and conduction band bottom is touching each other at the Γ point. This originates from the two fold degeneracy of the E_u states at the Γ point. As discussed previously, E_u states are doubly degenerate in

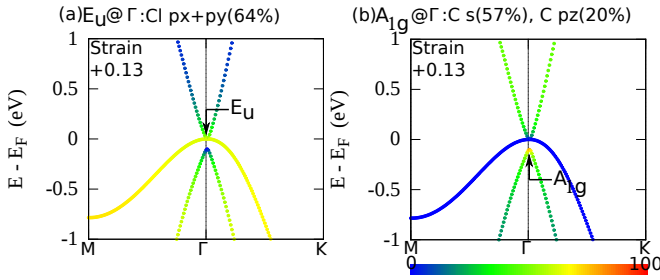


FIG. 4. Orbital resolved band structure of chlorographene under 13% tensile strain is shown in this figure. The valence and conduction band touches at the Γ point (zero bandgap) and chlorographene exists in semi-metallic state.

equilibrium (zero strain) also. It is not surprising that the degeneracy survives, because uniform biaxial strain does not change the symmetry of chlorographene. As shown in Fig. 4, energy level of E_u is higher than that of A_{1g} states, which is exactly opposite to what is observed in semiconducting state of chlorographene, i.e., in equilibrium (zero strain) and all the way to 12% tensile strain. At this critical value of strain, A_{1g} state drops below the energy level of E_u states, which marks the onset of semi-metallic state of chlorographene [also see Fig. 2]. Note that, in-between the semiconducting and semi-metallic phase, there might exist a triply degenerate state (two E_u and one A_{1g} state at the same energy level) at some particular value of strain, although it is difficult to identify it because DFT can not accurately predict bandgap smaller than a few milli-electron volt. On the other hand, semi-metallic state beyond 12% strain is very robust because it originates from the two fold degeneracy of the E_u states, protected by the symmetry of chlorographene. Based on the orbital resolved band structure shown in Fig. 4, it is also clear that the E_u (A_{1g}) states at the Γ point are mainly composed of p_x and p_y orbital of Cl (s and p_z orbital of C), which is consistent with the trend observed for chlorographene under tensile strain [see Fig. 3(e)].

Finally, we discuss the phase transition under compression and as mentioned previously, it is qualitatively different from the transition taking place under tensile strain [also see Fig. 2]. Finer details are illustrated in Fig. 5 (a) and (b), where electronic bands of chlorographene under 7% compressive strain are plotted along various high symmetry lines. Again, since uniform biaxial strain preserves the symmetries of chlorographene crystal, the doubly degenerate E_u states at the Γ point persists and have higher energy than that of A_{1g} states. Thus, similar to tensile strain, phase transition under compression also happens as the energy of A_{1g} drops below that of E_u states [see Fig. 2]. Orbital resolved band structure shown in Fig. 5 (a) and (b) also reveals that the E_u (A_{1g}) states at the Γ point are mainly composed of p_x and p_y orbital of Cl (p_z orbital of Cl and p_z orbital of C), which is consistent with the trend observed for chlorographene under compressive strain [see Fig. 3(e)]. Note that, neither

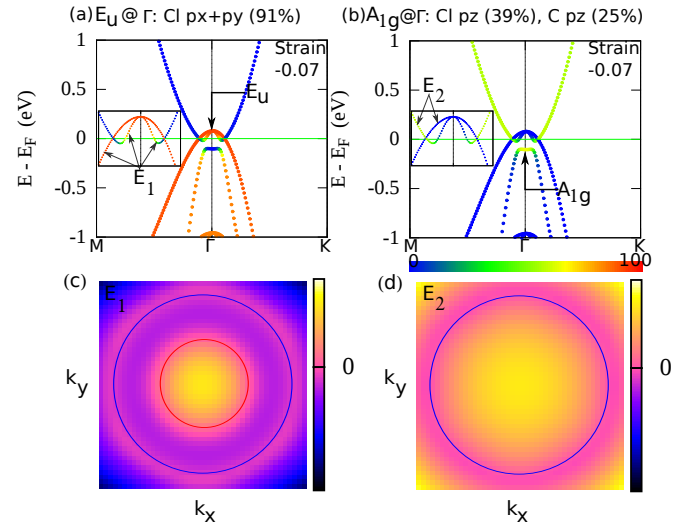


FIG. 5. Orbital resolved band structure of metallic chlorographene (under 7% compressive strain) is shown in (a) and (b). Relevant portion of the two bands (at the Fermi level) are magnified and shown in the insets. Band diagrams illustrated in the insets of (a) and (b) are further represented by surface plots of (c) $E_1(k_x, k_y)$ and (d) $E_2(k_x, k_y)$, where $E_2 \geq E_1$ at a reciprocal lattice point (k_x, k_y) . Since E_1 and E_2 are calculated with respect to the E_F , Fermi level lies along the zero energy contour lines, illustrated by the blue and red circle. Two bands cross along the outer blue circle, as shown in panel (c) and (d). The inner red circle of panel (c) is the other zero energy contour line, related to the partially filled band of chlorographene.

E_u , nor A_{1g} states at the Γ point are at the Fermi level, which lies in between the two [see Fig. 5(a) and (b)]. This leads to a partially filled band and consequently chlorographene transforms from semiconducting to a metallic state. Note that, Fermi level crosses the energy bands in two distinct places between ΓM , as well as ΓK [see insets of Fig. 5 (a) and (b)]. This is further elucidated by using surface plots of $E_1(k_x, k_y)$ and $E_2(k_x, k_y)$, where $E_2 \geq E_1$ at a reciprocal lattice point (k_x, k_y) [see Fig. 5(c)-(d)]. Fermi energy (zero energy contour line) lies along the red and blue circle, as shown in Fig. 5(c) and (d). Among the two, the outer circle (blue) has very interesting feature, with two energy bands crossing each other along the line. The inner red circle in Fig. 5(c) originates from the partially filled band [see Fig. 5(a)] and shows the location of the points where Fermi energy crosses $E_1(k_x, k_y)$.

So far our calculations do not include the effect of spin-orbit coupling. This is known to lift the degeneracy and induce energy gaps, especially at the high-symmetry points, in other 2D material like graphene.³⁹ As discussed previously, the two p orbitals of Cl, which makes the VBM of chlorographene (when it is a semiconductor), are degenerate at the Γ point [see Fig 1 and Fig 3]. However, once the spin-orbit coupling⁴⁰ is turned on, the degeneracy of the E_u states is lifted at the Γ point and the energy levels are split by a small margin of 20–40 meV. This is observed irrespective of the magnitude of the ap-

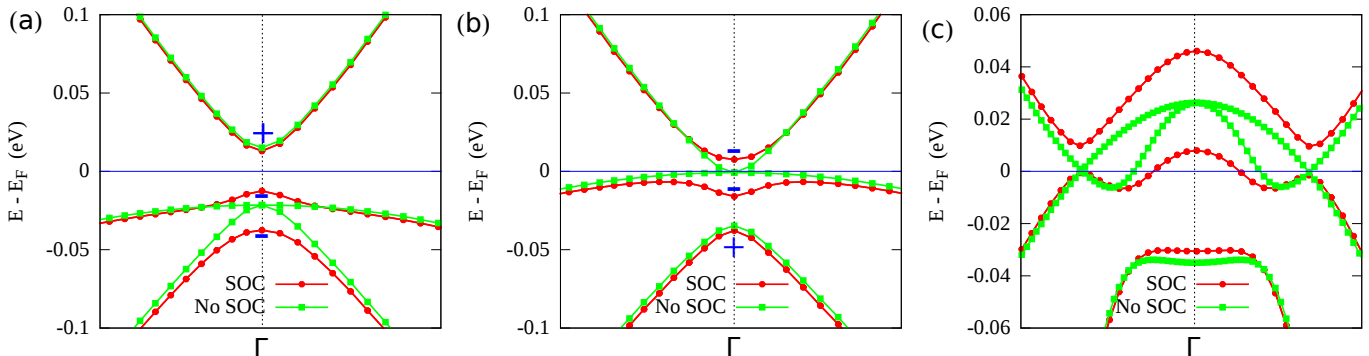


FIG. 6. Effect of spin-orbit coupling (SOC) on electronic band structure of chlorographene is shown for (a) 11% tensile, (b) 13% tensile and (c) 7% compressive strain. Clearly, degeneracy of the E_u states at the Γ point is lifted and a gap of magnitude 20 and 40 meV is created, in case of tensile and compressive strain, respectively. Additionally, in case of chlorographene under 7% compressive strain, a 10 meV energy gap is opened along the outer blue circle, where two bands were touching each other [see Fig. 5]. In panel (a) and (b), parities of the Bloch states at the Γ point are labeled by + and -.

plied strain, including the equilibrium (i.e., zero strain) state, as all of them have same space group symmetry. Three different cases are illustrated in Fig. 6: (a) 11% and (b) 13% stretched, which is before and after transition under tensile strain and (c) 7% squeezed, which is beyond the transition point under compressive strain. Interestingly, what appeared as a semi-metallic state of chlorographene beyond 12% tensile strain; after inclusion of spin-orbit coupling, turns out to be a semiconducting phase with a vanishingly small bandgap, measuring ~ 20 meV [see Fig. 6 (b)]. Further, comparing panel (a) and (b) of Fig. 6, a parity exchange between the occupied and unoccupied bands is observed at the Γ point. This type of parity change is known to be associated with topological phase transition.⁴¹ The metallic phase of chlorographene, which appears beyond 6.2% compressive strain, remains as it is even with spin-orbit coupling, because of the partially filled band [see Fig. 6(c)]. However, a small energy gap (~ 10 meV) opens along the outer blue circle [see Fig. 5 (c) and (d) and compare with Fig. 6(c)] due to the spin-orbit coupling.

Note that, bandgap values reported in this work are obtained from DFT-GGA calculations, which is known to underestimate its magnitude. As reported in the literature, using rigorous GW many-body perturbation theory method, bandgap of chlorographene (DFT-GGA estimate equal to 1.5 eV) was found to increase dramatically to a range of 4.3 to 4.9 eV.^{19,42} However, GW correc-

tion generally overestimates the bandgap.⁴³ For example, experimental bandgap of fluorographene lies in the range of 3 to 3.8 eV, but GW calculations predict it to be around 7 to 8 eV, while the DFT-GGA predictions are very close to the experimental value.⁴² However, even a 50-60% increase of bandgap of chlorographene is only going to enhance the strain at which the transformations are observed, while the results reported in this paper remains qualitatively same.

In conclusion, we show that chlorographene, which has a sizeable bandgap, can be driven to a state of vanishingly small bandgap or even a metal, by applying external strain. The semiconductor to metal transition takes place under compression, while tensile strain reduces the bandgap to a vanishingly small value of a few meV. Two bands are also found to be touching each other (at certain points lying on a circle surrounding the Γ point in the Brillouin zone) under sufficiently large compression, although they split marginally due to spin-orbit coupling.

I. ACKNOWLEDGEMENTS

SB acknowledges funding from SERB Fast Track Scheme for Young Scientist (SB/FTP/ETA-0036/2014). We also thank CC IITK for providing HPC facility.

* spuri@iitk.ac.in

† bsomnath@iitk.ac.in

¹ Ganesh R. Bhimanapati, Zhong Lin, Vincent Meunier, Yeonwoong Jung, Judy Cha, Saptarshi Das, Di Xiao, Youngwoo Son, Michael S. Strano, Valentino R. Cooper, Liangbo Liang, Steven G. Louie, Emilie Ringe, Wu Zhou, Steve S. Kim, Rajesh R. Naik, Bobby G. Sumpter, Humberto Terrones, Fengnian Xia, Yeliang Wang, Jun Zhu, Deji Akinwande, Nasim Alem, Jon A. Schuller, Ray-

mond E. Schaak, Mauricio Terrones, and Joshua A. Robinson, "Recent advances in two-dimensional materials beyond graphene," *ACS Nano* **9**, 11509–11539 (2015)

² K. S. Novoselov, A. K. Geim, S. V. Morozov, D. Jiang, Y. Zhang, S. V. Dubonos, I. V. Grigorieva, and A. A. Firsov, "Electric field effect in atomically thin carbon films," *Science* **306**, 666–669 (2004)

³ K. S. Novoselov, D. Jiang, F. Schedin, T. J. Booth, V. V. Khotkevich, S. V. Morozov, and A. K. Geim, "Two-

- dimensional atomic crystals,” *Proceedings of the National Academy of Sciences of the United States of America* **102**, 10451–10453 (2005)
- 4 Andre K Geim and Konstantin S Novoselov, “The rise of graphene,” *Nat. Mater.* **6**, 183–191 (2007)
 - 5 P. R. Wallace, “The band theory of graphite,” *Phys. Rev.* **71**, 622–634 (1947)
 - 6 A. H. Castro Neto, F. Guinea, N. M. R. Peres, K. S. Novoselov, and A. K. Geim, “The electronic properties of graphene,” *Rev. Mod. Phys.* **81**, 109–162 (2009)
 - 7 Young-Woo Son, Marvin L. Cohen, and Steven G. Louie, “Energy gaps in graphene nanoribbons,” *Phys. Rev. Lett.* **97**, 216803 (2006)
 - 8 Y.-W. Son, M. L. Cohen, and S. G. Louie, “Half-metallic graphene nanoribbons,” *Nature (London)* **444**, 347–349 (2006), [cond-mat/0611600](#)
 - 9 Somnath Bhowmick and Vijay B. Shenoy, “Weber-fechner type nonlinear behavior in zigzag edge graphene nanoribbons,” *Phys. Rev. B* **82**, 155448 (2010)
 - 10 Somnath Bhowmick, Amal Medhi, and Vijay B. Shenoy, “Sensory-organ-like response determines the magnetism of zigzag-edged honeycomb nanoribbons,” *Phys. Rev. B* **87**, 085412 (2013)
 - 11 Marcel H. F. Sluiter and Yoshiyuki Kawazoe, “Cluster expansion method for adsorption: Application to hydrogen chemisorption on graphene,” *Phys. Rev. B* **68**, 085410 (2003)
 - 12 Jorge O. Sofo, Ajay S. Chaudhari, and Greg D. Barber, “Graphane: A two-dimensional hydrocarbon,” *Phys. Rev. B* **75**, 153401 (2007)
 - 13 Jeremy T. Robinson, James S. Burgess, Chad E. Junkermeier, Stefan C. Badescu, Thomas L. Reinecke, F. Keith Perkins, Maxim K. Zalalutdinov, Jeffrey W. Baldwin, James C. Culbertson, Paul E. Sheehan, and Eric S. Snow, “Properties of fluorinated graphene films,” *Nano Letters* **10**, 3001–3005 (2010)
 - 14 Rahul R. Nair, Wencai Ren, Rashid Jalil, Ibtisam Riaz, Vasyl G. Kravets, Liam Britnell, Peter Blake, Fredrik Schedin, Alexander S. Mayorov, Shengjun Yuan, Mikhail I. Katsnelson, Hui-Ming Cheng, Wlodek Strupinski, Lyubov G. Bulusheva, Alexander V. Okotrub, Irina V. Grigorieva, Alexander N. Grigorenko, Kostya S. Novoselov, and Andre K. Geim, “Fluorographene: A two-dimensional counterpart of teflon,” *Small* **6**, 2877–2884 (2010)
 - 15 Radek Zboil, Frantiek Karlick, Athanasios B. Bourlinos, Theodore A. Steriotis, Athanasios K. Stubos, Vasilios Georgakilas, Klara afov, Dalibor Jank, Christos Trapalis, and Michal Otyepka, “Graphene fluoride: A stable stoichiometric graphene derivative and its chemical conversion to graphene,” *Small* **6**, 2885–2891 (2010)
 - 16 F. Withers, M. Dubois, and A. K. Savchenko, “Electron properties of fluorinated single-layer graphene transistors,” *Phys. Rev. B* **82**, 073403 (2010)
 - 17 Bo Li, Lin Zhou, Di Wu, Hailin Peng, Kai Yan, Yu Zhou, and Zhongfan Liu, “Photochemical chlorination of graphene,” *ACS Nano* **5**, 5957–5961 (2011)
 - 18 Joelson C. Garcia, Denille B. de Lima, Lucy V. C. Assali, and Joo F. Justo, “Group iv graphene- and graphane-like nanosheets,” *The Journal of Physical Chemistry C* **115**, 13242–13246 (2011)
 - 19 H. Sahin and S. Ciraci, “Chlorine adsorption on graphene: Chlorographene,” *The Journal of Physical Chemistry C* **116**, 24075–24083 (2012)
 - 20 Hiram J. Conley, Bin Wang, Jed I. Ziegler, Richard F. Haglund, Sokrates T. Pantelides, and Kirill I. Bolotin, “Bandgap engineering of strained monolayer and bilayer mos2,” *Nano Letters* **13**, 3626–3630 (2013)
 - 21 David Lloyd, Xinghui Liu, Jason W. Christopher, Lauren Cantley, Anubhav Wadehra, Brian L. Kim, Bennett B. Goldberg, Anna K. Swan, and J. Scott Bunch, “Band gap engineering with ultralarge biaxial strains in suspended monolayer mos2,” *Nano Letters* **16**, 5836–5841 (2016)
 - 22 Zhen Zhu and David Tománek, “Semiconducting layered blue phosphorus: A computational study,” *Phys. Rev. Lett.* **112**, 176802 (2014)
 - 23 Jie Guan, Zhen Zhu, and David Tománek, “Phase coexistence and metal-insulator transition in few-layer phosphorene: A computational study,” *Phys. Rev. Lett.* **113**, 046804 (2014)
 - 24 Ruixiang Fei and Li Yang, “Strain-engineering the anisotropic electrical conductance of few-layer black phosphorus,” *Nano Letters* **14**, 2884–2889 (2014)
 - 25 Ning Lu, Hongyan Guo, Lei Li, Jun Dai, Lu Wang, Wai-Ning Mei, Xiaojun Wu, and Xiao Cheng Zeng, “Mos2/mx2 heterobilayers: bandgap engineering via tensile strain or external electrical field,” *Nanoscale* **6**, 2879–2886 (2014)
 - 26 Jingshan Qi, Xiao Li, Xiaofeng Qian, and Ji Feng, “Bandgap engineering of rippled mos2 monolayer under external electric field,” *Applied Physics Letters* **102**, 173112 (2013)
 - 27 Qihang Liu, Linze Li, Yafei Li, Zhengxiang Gao, Zhongfang Chen, and Jing Lu, “Tuning electronic structure of bilayer mos2 by vertical electric field: A first-principles investigation,” *The Journal of Physical Chemistry C* **116**, 21556–21562 (2012)
 - 28 Qihang Liu, Xiuwen Zhang, L. B. Abdalla, Adalberto Fazzio, and Alex Zunger, “Switching a normal insulator into a topological insulator via electric field with application to phosphorene,” *Nano Letters* **15**, 1222–1228 (2015)
 - 29 Jun Dai and Xiao Cheng Zeng, “Bilayer phosphorene: Effect of stacking order on bandgap and its potential applications in thin-film solar cells,” *The Journal of Physical Chemistry Letters* **5**, 1289–1293 (2014)
 - 30 Dong Li, Jin-Rong Xu, Kun Ba, Ningning Xuan, Mingyuan Chen, Zhengzong Sun, Yu-Zhong Zhang, and Zengxing Zhang, “Tunable bandgap in few-layer black phosphorus by electrical field,” *2D Materials* **4**, 031009 (2017)
 - 31 Barun Ghosh, Suhas Nahas, Somnath Bhowmick, and Amit Agarwal, “Electric field induced gap modification in ultrathin blue phosphorus,” *Phys. Rev. B* **91**, 115433 (2015)
 - 32 Kechao Tang, Rui Qin, Jing Zhou, Heruge Qu, Jiabin Zheng, Ruixiang Fei, Hong Li, Qiye Zheng, Zhengxiang Gao, and Jing Lu, “Electric-field-induced energy gap in few-layer graphene,” *The Journal of Physical Chemistry C* **115**, 9458–9464 (2011)
 - 33 Anton Kokalj, “Computer graphics and graphical user interfaces as tools in simulations of matter at the atomic scale,” *Computational Materials Science* **28**, 155 – 168 (2003), proceedings of the Symposium on Software Development for Process and Materials Design
 - 34 Anton Kokalj, “Xcrysdena new program for displaying crystalline structures and electron densities,” *Journal of Molecular Graphics and Modelling* **17**, 176 – 179 (1999)
 - 35 Paolo Giannozzi, Stefano Baroni, Nicola Bonini, Matteo Calandra, Roberto Car, Carlo Cavazzoni, Davide Ceresoli, Guido L Chiarotti, Matteo Cococcioni, Ismaila Dabo, An-

- drea Dal Corso, Stefano de Gironcoli, Stefano Fabris, Guido Fratesi, Ralph Gebauer, Uwe Gerstmann, Christos Gougoussis, Anton Kokalj, Michele Lazzeri, Layla Martin-Samos, Nicola Marzari, Francesco Mauri, Riccardo Mazzarello, Stefano Paolini, Alfredo Pasquarello, Lorenzo Paulatto, Carlo Sbraccia, Sandro Scandolo, Gabriele Scaluzero, Ari P Seitsonen, Alexander Smogunov, Paolo Umari, and Renata M Wentzcovitch, “Quantum espresso: a modular and open-source software project for quantum simulations of materials,” *Journal of Physics: Condensed Matter* **21**, 395502 (19pp) (2009)
- ³⁶ Point group symmetry of the wave vector \mathbf{k} at the Γ , K and M point is D_{3d} , D_3 and C_{2h} , respectively and along the Γ -K, K-M and M- Γ line is C_2 , C_2 and C_s , respectively.
- ³⁷ Sougata Mardanya, Vinay Kumar Thakur, Somnath Bhowmick, and Amit Agarwal, “Four allotropes of semiconducting layered arsenic that switch into a topological insulator via an electric field: Computational study,” *Phys. Rev. B* **94**, 035423 (2016)
- ³⁸ Liyan Zhu, Shan-Shan Wang, Shan Guan, Ying Liu, Tingting Zhang, Guibin Chen, and Shengyuan A. Yang, “Blue phosphorene oxide: Strain-tunable quantum phase transitions and novel 2d emergent fermions,” *Nano Letters* **16**, 6548–6554 (2016)
- ³⁹ Sergej Konschuh, Martin Gmitra, and Jaroslav Fabian, “Tight-binding theory of the spin-orbit coupling in graphene,” *Phys. Rev. B* **82**, 245412 (2010)
- ⁴⁰ Fully relativistic pseudopotentials are used for spin-orbit coupling calculations.
- ⁴¹ Liang Fu and C. L. Kane, “Topological insulators with inversion symmetry,” *Phys. Rev. B* **76**, 045302 (2007)
- ⁴² Frantiek Karlick and Michal Otyepka, “Band gaps and optical spectra of chlorographene, fluorographene and graphane from g0w0, gw0 and gw calculations on top of pbe and hse06 orbitals,” *Journal of Chemical Theory and Computation* **9**, 4155–4164 (2013)
- ⁴³ Jason M. Crowley, Jamil Tahir-Kheli, and William A. Goddard, “Resolution of the band gap prediction problem for materials design,” *The Journal of Physical Chemistry Letters* **7**, 1198–1203 (2016)